Available online at www.sciencedirect.com

ScienceDirect

IFAC PapersOnline CONFERENCE PAPER ARCHIVE

IFAC PapersOnLine 55-5 (2022) 43–48

Integrating local and global projections for the generation of water demand scenarios in the Red River Basin, Vietnam

Michele Mauri * **Kushagra Pandey** * **Matteo Giuliani** * **Andrea Castelletti** *

* *Department of Electronics, Information, and Bioengineering, Politecnico di Milano, Via Ponzio 34/5, 20133 Milano, Italy (e-mail: michele1.mauri@polimi.it, kushagra.pandey@mail.polimi.it, matteo.giuliani@polimi.it, andrea.castelletti@polimi.it)*

Abstract: Planning and management of water supply systems require projections to account for future changes in climate and society. Global and local future scenarios are generated by using models at different spatial scales. The choice of the scale affects if and how the regional socio-economic structure as well as global and local development strategies are considered, and which uncertainties are treated explicitly. This study explores the integration of global and local scale scenarios. Our approach is demonstrated on the Red River basin, Vietnam, where a set of plausible water demands scenarios is generated for 2050. Results show that water demand will increase by 28-58% compared to 2010 when considering all scenarios of climate and socio-economic changes. The ensemble of integrated demands shows a strong dependence of water demand upon the climate-socio-economic state, which allow a better characterization of the future water supply sector dynamics than those obtained by global or local projections only.

Copyright © 2022 The Authors. This is an open access article under the CC BY-NC-ND license (https://creativecommons.org/licenses/by-nc-nd/4.0/)

Keywords: Water demand, Scenario generation, Uncertainty, Red River basin.

1. INTRODUCTION

New infrastructures and management strategies that will satisfy future societal needs strongly depend on the co-evolution of Humans and the climate system (Alcamo et al., 2007; Arnell, 2004). This evolution is affected by deep uncertainty, implying that a single trajectory is not enough to fully characterize the futures state of the climate and the socio-economic system (Lempert, 2002). Deep uncertainty has implications for future infrastructure resilience and its capacity of providing adequate service during this century and should be, therefore, considered in designing adaptation strategies that are robust across a wide range of plausible futures (Herman et al., 2020).

Numerical models have been developed for the exploration of socio-economic and environmental dynamics and scenarios (Vinca et al., 2021). Two standard methodologies are used for the generation of scenarios. According to the global (top-down) approach, global models are run and then downscaled to a smaller scale to assess the impacts in the area of interest (Bosshard et al., 2014; Gusain et al., 2020). This method applies also to the assessment of Shared Socio-economic Pathways (SSPs) (O'Neill et al., 2017; Riahi et al., 2017) and Representative Concentration Pathways (RCPs) (Van Vuuren et al., 2011). Those narratives describe independent and plausible trajectories for the socio-economic variables (SSPs), including population and GDP, and the radiative forcing (RCPs). Alternatively, the local (bottom-up) approach recommends constructing regional scenarios with local models exploiting local characteristics and development pathways. Possible applications of the local methodology include assessment of adaptation capabilities and vulnerabilities in the water supply system (Culley et al., 2016). Local scenarios might be generated assuming development trajectories defined by stakeholders while overlooking the influence of global factors such as climate (Herman et al., 2014). Hence, local scenarios are in some sense independent of the global dynamics but have the advantage that can describe peculiar societal-environmental features, which might be unexploited by large scale models.

Recent advances in the field of Integrated Assessment Models (IAMs) have given researchers the opportunity to explore the dynamics and interactions at a global scale of socio-economic and environmental variables (Garner et al., 2016). They can project variables tracking different world regions under a predefined socio-economic trajectory (usually one of the SSPs), with negligible or limited feedback from the climate system. IAMs hence observe socio-economic evolution from a global perspective and, by applying downscaling, their scenarios can be used in local impact estimation. SSPs can be linked to RCPs and assessed to simultaneously produce global scenarios that are consistent from the socio-economic and climatic perspectives.

In this work, we focus on integrating local and global scenarios for the generation of future projections of multisector water demand and apply our method to the case study of the Red River Basin (RRB) in Vietnam. In a rapidly evolving context such as the RRB, recognizing the future uncertainty is crucial to explore how the space of

2405-8963 Copyright © 2022 The Authors. This is an open access article under the CC BY-NC-ND license.
Peer review under responsibility of International Federation of Automatic Control.
10.1016/j.ifacol.2022.07.637

transformations will shape (Giuliani et al., 2016). At the same time, it is important to identify the factors relevant to the evolution of water demand since their alteration could expose the basin to water supply stresses or trigger the deployment of adaptation or mitigation measures. This work is motivated by the recognition that a gap exists between local and global generation methodologies, the first being able to exploit the regional socio-economic structure of the society and follow local future development pathways at better resolution, the latter being able to produce downscaled but globally consistent scenario of alternative futures. We therefore propose integrating global and local scale scenarios of water demand to complement information that emerges from different scales to produce a set of water demands that simultaneously address the complexity of the global socio-economic evolution, the changing climate conditions, and local features and development trajectories. The final set of scenarios obtained through scale integration is able to span the range of uncertainties and is ready to be used to assess impacts and adaptation strategies while considering climate-socio-economic interdependent scenarios and the different drivers of change.

2. THE RED RIVER BASIN

The Red River Basin is a transnational basin covering an area of 169,000 km^2 between Vietnam (51.3%), China (48%), and Laos (0.7%), the second-largest basin in the country after the Mekong. The three main tributaries of the Red River (Da, Lo, and Thao) rise in the northern part of the basin and join before reaching the large flood plain in the delta region, which extends over 21,000 km^2. The basin is characterized by a tropical monsoon climate. The Red River Delta (RRD) is an area of rapid socio-economic transformation, where different sectors (agriculture, industry, and urbanization) compete for resources such as water and land. Nonetheless, agriculture remains the main economic activity, accounting for 58% of the total water demand and involving around 50% of the local workers in 501,000 *ha* of cultivated fields. Rice cultivation in the RRB (along with the Mekong basin) makes Vietnam the second-largest rice exporter in the world (Yu et al., 2010). Aquaculture is the second water consumer in the basin (29%). The delta is undergoing an expansion of aquaculture, which is water-intensive and performed in small inland ponds or along the coastline. Moreover, the processes of urbanization and industrial expansion (Fox et al., 2018) increase, even more, the pressure on the water supply system in the delta. Finally, climate change is expected to affect the Vietnamese economy (Arndt et al., 2015) in the future, thus calling for a better understanding of climate change consequences (e.g., changes in precipitations).

3. MODELS AND METHODS

The workflow (Fig. 1) shows the process of generation of local and global water demands. Initially, a weather generator is trained on historical data. Then, synthetically generated trajectories are perturbed to represent alternative states of the climate in the basin and used to compute agriculture and aquaculture water demands. The locally-generated demands are subsequently linked to RCPs considering the underlying state of the climate generating each

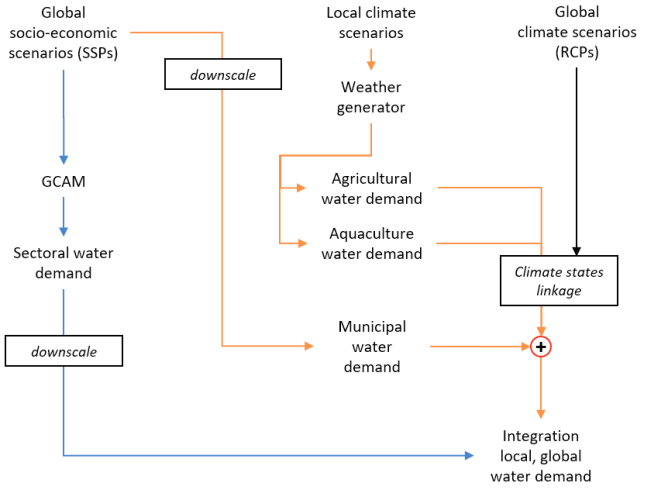

Fig. 1. Workflow for this study. Blue arrows indicate the steps for the generation of water demand with a global model. In orange, the generation of the demand via local modeling. Black boxes represent intermediate processing steps.

demand. Secondly, we extract and downscale from SSPs to basin resolution global population and urbanization rates, which are used to compute municipal water demand locally. Finally, the GCAM model (see section 3.4) is run under each SSP-baseline scenario and later downscaled to obtain water demand for each sector. Local and global (GCAM) demands are finally integrated to exploit information from local and global scales simultaneously.

3.1 Climate scenarios

Temperature and precipitation scenarios for the basin are produced in two steps. First, historical climate trajectories are used in the calibration of a semi-parametric weather generator (Wilks and Wilby, 1999) able to produce statistically equivalent weather trajectories. Then, the generated time series are perturbed to simulate alternative states of the climate system. The Vietnamese government provided historical climate data (temperature and precipitation) for the period 1961-2000 for five meteorological stations (Do, Gam, La, Thai, Chay) placed along the main rivers in the Red River Basin. The weather generator is run to obtain a set of 56 synthetic time series (40 years each) of temperature and precipitation. The generated trajectories keep the seasonal characteristics of the historical records and preserve the spatial correlation among the five meteorological stations. Perturbations are applied to the time-series using additive (for temperature) and multiplicative (for precipitation) coefficients in order to generate alternative mild to extreme climate scenarios. The additive coefficients vary from -2°C to +5°C with a 1°C step, while the multiplicative coefficient spans 0.8 to 1.6 with a 0.1 step.

3.2 Local water demand

Locally generated water demand is made up of three components: agricultural, aquaculture and municipal, the first two depending on the state of the climate and the latter driven by the socio-economic assumptions. Alternative climate states were used to assess changes in the agricultural

and aquaculture water demand. Downscaled SSPs were used to quantify municipal water demand in 2050.

Agriculture water demand We compute agriculture water demand for alternative climate states and the corresponding weather trajectories with the CROPWAT software (Smith, 1992). The calculation of the irrigation need is based on the water balance equation:

$$W^{irr} = ET_c + LP_{rep} + P_{rep} - P_{eff} \quad (1)$$

where the variables are the surface evapotranspiration ET_c, the amount of soil water LP_{rep}, the stability of groundwater P_{rep}, and the effective rainfall P_{eff}. Evapotranspiration is based on the Penman-Monteith equation, which requires weather data: temperature and precipitation are computed via the weather generator, others are measured on-site, such as wind speed and solar irradiance. The remaining variables are computed based on the crop distribution in the RRD and soil characteristics provided by the Vietnamese government.

Aquaculture water demand Aquaculture water demand is computed via the equation:

$$W^{aq} = EP_c + SP_{rep} - P \quad (2)$$

where EP_c is the surface evaporation loss in the aqua pond, SP_{rep} is the seepage loss, P is the precipitation of the day. Evaporative water loss is determined using ambient air temperature, humidity, and solar radiation (Valiantzas, 2006). Where available, as in equation (1), generated weather data were used to simulate altered historical conditions. The seepage loss is related to the soil type, assumed to be loamy.

Municipal water demand Municipal water demand is projected to 2050, taking into account the changes in the population of the basin and the migration from the rural to the urban areas, which implies a higher per capita water consumption. The municipal demand is computed using the equation:

$$W^{mun} = \sum_{area \in r,t,u} POP_{area} * PCC_{area} \quad (3)$$

where POP_{area} is the population living in rural, town or urban areas (respectively, r, t and u in equation (3)), PCC_{area} is the per-capita water consumption in each area. The Vietnamese government provided data relative to the basin's population and the share of rural, town and urban inhabitants in 2010. First, the total basin's population is computed by downscaling the projected Vietnam's population in 2050. Then, it is multiplied by the 2050 urbanization coefficient (Jiang and O'Neill, 2017), which distinguishes only between rural and urban areas. Finally, POP_{area} is computed for each segment by differentiating town and urban inhabitants. The standards of water consumption PCC_{area} in 2050 are assumed to equal the per-capita water consumption in 2010 since the latter is the most recent data provided by Vietnam's government.

3.3 Climate states linkage to RCP

For local scenarios, we link climate states to RCP by comparing the set of perturbed temperatures and precipitations with projections from 34 different General Circulation Models (GCM) in the CMIP5 multimodel ensemble run with starting conditions selected across all four RCPs (Quinn et al., 2018). We manually select for each RCP a set of climate states, which is compatible with GCMs' projections. Then, climate dependent water demands projections are aggregated by RCPs in order to have a more compact representation of the plausible demand changes under scenarios of climate change while avoiding extreme and unlikely climate conditions.

3.4 The GCAM model

The Global Change Assessment Model (GCAM) (Calvin et al., 2019) is a global scale, open-source model that represents the linkages between energy, water, land, climate, and economic systems. It can be used to examine, for example, how changes in population, income, or technology cost might alter crop production, energy demand, or water withdrawals, or how changes in one region's demand for energy affect energy, water, and land in other regions. In GCAM three distinct sources of freshwater are modelled: renewable water (surface and ground), non-renewable groundwater, and desalinated water. Water withdrawals and consumption are tracked for six sectors (irrigation, electricity, municipal, industrial, mining, and livestock) over all regions. In this work, GCAM it is used to project to 2050 SSP trajectories to calculate the water demand for the macro-region which includes the RRB. Water withdrawals are not considered in the analysis.

3.5 Global downscaled water demand

GCAM was run under all five SSP-baseline scenarios (no additional policies or constraints on the radiative forcing). The RRB is included in a larger region, so a downscale proportional to the historical (2010) water consumption was applied. Data projected to 2050 were downscaled to the level of the RRB for all sectors.

3.6 Integrated local-global water demand

The integration process generates a set of alternative water demands maximizing the information on the evolution of the different sectors in the basin. Agricultural and municipal demands, both locally and globally projected, are compared to verify that there are no inconsistencies across scales. Integrated local-global water demands are created by summing up sectors and exploring the different climate and socio-economic couplings. In particular, only the SSP-RCP combinations which have been assessed with IAMs are considered (Riahi et al., 2017). The set of demands fulfils the sector gaps which had existed if only local or global projections had been used and it is consistent across scales and climate-socio-economic scenarios.

4. RESULTS

We present at first water demand projections in 2050 for the RRB for the local generation process (agricultural, aquaculture and municipal sectors). Then, we report global demands generated through GCAM and downscaled

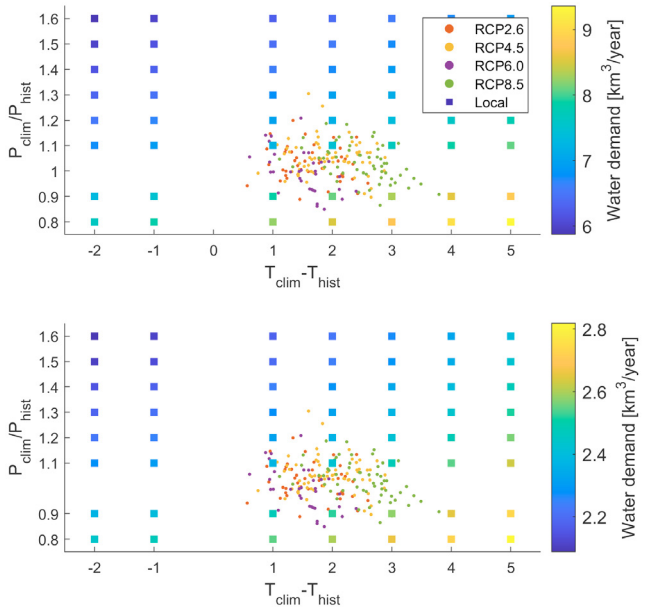

Fig. 2. Agriculture (top) and aquaculture (bottom) locally generated water demands. Each square represents one of the 56 local climate states and its color gradient depends on the associated water demand. Colored dots indicate climate projections by GCMs in 2050, each color referring to a different RCP. Temperature shifts are reported on the x-axis, precipitation coefficients on the y-axis.

to the basin. Finally, we show the result of the integration procedure and the set of the resulting locally-globally consistent demand scenarios.

4.1 Locally generated water demand

Agriculture and aquaculture demand The agricultural and aquaculture demands are reported in Fig. 2 for the 56 climate state. The range of the predicted demand is large and depends on the underlying climate condition. In the case of agriculture, a minimum of 5.9 km^3/yr is reached for the lowest temperature, highest precipitation scenario; conversely, when the temperature is maximum and precipitation is minimum, the demand increases up to 9.4 km^3/yr. Similar behavior is observed also for aquaculture, with the demand spanning between 2.1 and 2.8 km^3/yr. The relation between the temperature, precipitation and water demand observable in the result is the outcome of how the demand is modelled (equation (1) and (2)).

Municipal demand The municipal water demand differs across SSPs given the different assumptions on population and urbanization rates. Water demand is the highest for SSP1 (1.82 km^3/yr), the lowest for SSP3 (1.58 km^3/yr). The remaining projections are closer to SSP1 and stand at 1.80 km^3/yr (SSP4), 1.79 km^3/yr (SSP5) and 1.71 km^3/yr (SSP1). Considering all pathways, urban water demand accounts for 50-70% of the total, followed by rural (15-37%) and town (12-17%).

4.2 Linkage to RCP scenarios

The superimposition of the GCMs' projections on the grid of temperature and precipitation perturbation allows

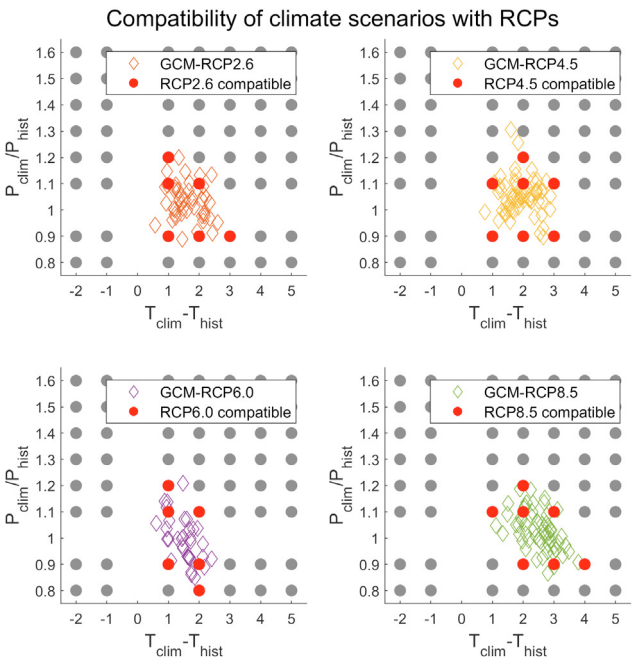

Fig. 3. Diamonds represent climate projections by GCMs in 2050. Grey dots are climate states simulated in the local generation process, while red dots identify the local climate conditions which match global scale projections. Same axes as in Fig. 2

the selection of four subsets of climate states which are compatible with each climate pathway (Fig. 3). RCP2.6 is linked with n=6 local climate scenarios; for the other RCPs, the number is similar: RCP4.5 (n=7), RCP6.0 (n=6), RCP8.5 (n =7). The most extreme climate scenarios which are associated to any RCP are +2°C temperature increase, +20% precipitations change (RCP4.5), +2°C,-20% (RCP6.0) and +4°C,+10% (RCP8.5). The subsets overlap, but each contains at least one unique climate state (i.e., not included in the other subsets).

4.3 GCAM water demand

The projected GCAM water demand for 2050 in the basin is maximum for the SSP5 at 15.0 km^3/yr. The minimum is reached for SSP3 (12.7 km^3/yr). Alternative pathways report a demand of 13.0 km^3/yr (SSP4), 13.6 km^3/yr (SSP1) and 13.7 km^3/yr (SSP2). Even in the absence of aquaculture (not modelled in GCAM), food production remains the largest water consumer (47-55%), followed by electricity (14-20%), industrial (14-17%) and municipal (13-14%). In terms of absolute demand, municipal (+64%) and industry (+194%) have increased substantially compared to 2010. We cannot make the same comparison for electricity, having no official data. Livestock and mining compartment remains almost negligible, with an aggregate share lower than 3% across all SSPs.

4.4 Integration of local and global demands

Local-global consistency The global demand for agriculture underestimates the local one. The range of the GCAM projections is 6.5-7.4 km^3/yr, the highest corresponding to SSP1 and the lowest to SSP3. Conversely, among local

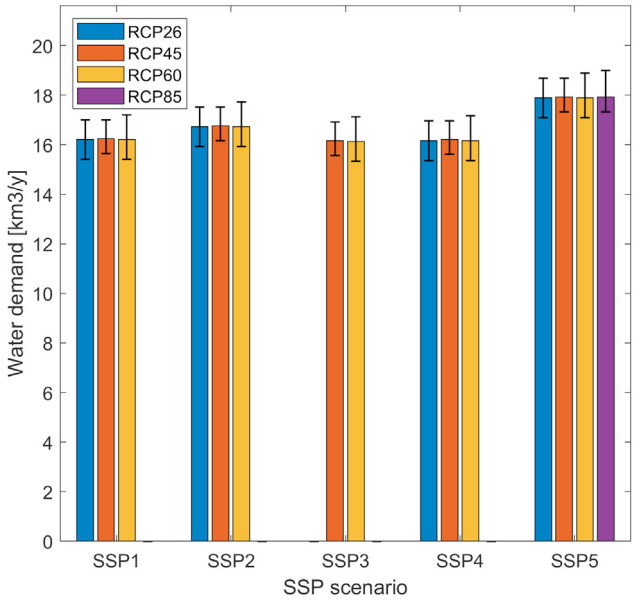

Fig. 4. Total water demand in the basin projected in 2050. Groups of bars refer to different SSPs. Height and whiskers of the bars represent, respectively, the median and the range of the water demand estimated considering the local climate states matching a given RCP.

demands, the lowest is 7.0 km^3/yr (RCP2.6 and RCP6.0), the highest equals 8.6 km^3/yr (RCP8.5). Municipal demand can be compared directly across SSPs for the local and the global generation processes. The difference in the demand is maximum for SSP4, in which the local demand ($2.0km^3/yr$) is higher than the GCAM projected demand ($1.8km^3/yr$). The difference between the two generation methods is small (10%) and even narrower in the other SSPs (albeit not in all scenarios the local demand is higher than the global). Since there are no large differences between global and local demands, we can safely assume the latter as the reference for the generation of the integrated scenarios.

Aggregated water demand The combination of SSPs and RCPs led to 15 climate-socio-economic scenarios (Fig. 4). The projected total water demand for the RRB in 2050 is between 15.3 and 19.0 km^3/yr. Among socio-economic scenarios, SSP5 is the one associated with the highest demand (median 17.9 km^3/yr), substantially larger than the others, followed by SSP2 at 16.7 km^3/yr. The remaining SSPs project similar demands (median 16.2 km^3/yr). Across sectors, agriculture is the main consumer (43-48%), followed by aquaculture (14-15 %). Industrial (12-14%), municipal (10-11%) and electricity 11-17% demands account for 10-13% each, while the remaining sectors (primary and livestock) occupy the remaining share ($< 3\%$). Climate conditions influence the total demand, even though alternative RCPs do not cause a substantial difference in the median demand. The main impact of the climate is to cause an additional fluctuation, to each SSPs' demand, between -4% and +7%.

5. DISCUSSION AND CONCLUSION

The projected water demand for 2050 in the RRB shows that the area is going to strongly increase its water demand. As a reference, the total demand in the basin was 12 km^3/yr in 2010 compared to 15.3-19.0 km^3/yr projected in 2050. The integrated scenarios shows that both climate and socio-economic changes affect the range of demand and act as a source of uncertainty. Nonetheless, SSPs and RCPs play different roles. From one side, SSPs are a driver of the demand capable of shifting the median estimate. In particular, SSP5 is significantly higher than all the other scenarios. Conversely, the climate is a factor of uncertainty whose influence adds a range of variability without meaningful differences across RCPs. The roles of climate and socio-economic assumptions suggest that attention should be paid to the socio-economic development of the basin to avoid the stronger increase of the demand which could realize in certain conditions (e.g., SSP5). Also, since climate will influence the availability of water beside the demand, management and improvement of the water supply system could be needed to mitigate the impact of climate.

The methodology reported in this work shows that it is possible to combine scenarios from local and global projections. The method used to aggregate the climate perturbations is to superimpose GCM projections to obtain subsets of climate states compatible with the RCPs, and then the RCPs can be linked to alternative SSPs via the scenario matrix architecture (Van Vuuren et al., 2014). The resulting set (of subsets) allowed to explore the generated water demand for alternative climate-socio-economic states and assess the associated uncertainty and the level of impact of climate and socio-economic drivers on the demand. The use of local demand projection in addition to global projections could, in principle, allow the exploration of extreme scenarios of climate change. Also, compared to global projections, the local generation process has the advantage that can be tuned ad-hoc for the generation of sector demand non included in the global model (GCAM).

The integration process can surely be improved by increasing the detail in the sector description, which could include, in the case of RRB, water use for the environment which is relevant in the river delta but not modelled. The dependence of socio-economic variables in this work has been limited to the population and the urbanization share. Improvements are possible in this direction, for example by using different land-cover maps for agriculture and aquaculture to better describe the change of the economic structure over the future.

We think that the integration process shown in this work could help in filling the gap between global and local models, whose output should be consistent across scales. The method shown can be also applied to other river basins to build a set of future scenarios -even beyond water- which is more complete and informative than focusing only on one scale.

REFERENCES

Alcamo, J., Flörke, M., and Märker, M. (2007). Future long-term changes in global water resources driven by

socio-economic and climatic changes. *Hydrological Sciences Journal*, 52(2), 247–275.

Arndt, C., Tarp, F., and Thurlow, J. (2015). The economic costs of climate change: a multi-sector impact assessment for vietnam. *Sustainability*, 7(4), 4131–4145.

Arnell, N.W. (2004). Climate change and global water resources: Sres emissions and socio-economic scenarios. *Global environmental change*, 14(1), 31–52.

Bosshard, T., Kotlarski, S., Zappa, M., and Schär, C. (2014). Hydrological climate-impact projections for the rhine river: Gcm–rcm uncertainty and separate temperature and precipitation effects. *Journal of Hydrometeorology*, 15(2), 697–713.

Calvin, K., Patel, P., Clarke, L., Asrar, G., Bond-Lamberty, B., Cui, R.Y., Di Vittorio, A., Dorheim, K., Edmonds, J., Hartin, C., et al. (2019). Gcam v5. 1: representing the linkages between energy, water, land, climate, and economic systems. *Geoscientific Model Development*, 12(2), 677–698.

Culley, S., Noble, S., Yates, A., Timbs, M., Westra, S., Maier, H., Giuliani, M., and Castelletti, A. (2016). A bottom-up approach to identifying the maximum operational adaptive capacity of water resource systems to a changing climate. *Water Resources Research*, 52(9), 6751–6768.

Fox, J., Nghiem, T., Kimkong, H., Hurni, K., and Baird, I.G. (2018). Large-scale land concessions, migration, and land use: the paradox of industrial estates in the red river delta of vietnam and rubber plantations of northeast cambodia. *Land*, 7(2), 77.

Garner, G., Reed, P., and Keller, K. (2016). Climate risk management requires explicit representation of societal trade-offs. *Climatic Change*, 134(4), 713–723.

Giuliani, M., Anghileri, D., Castelletti, A., Vu, P.N., and Soncini-Sessa, R. (2016). Large storage operations under climate change: expanding uncertainties and evolving tradeoffs. *Environmental Research Letters*, 11(3), 035009.

Gusain, A., Mohanty, M., Ghosh, S., Chatterjee, C., and Karmakar, S. (2020). Capturing transformation of flood hazard over a large river basin under changing climate using a top-down approach. *Science of the Total Environment*, 726, 138600.

Herman, J.D., Quinn, J.D., Steinschneider, S., Giuliani, M., and Fletcher, S. (2020). Climate adaptation as a control problem: Review and perspectives on dynamic water resources planning under uncertainty. *Water Resources Research*, 56(2), e24389.

Herman, J.D., Zeff, H.B., Reed, P.M., and Characklis, G.W. (2014). Beyond optimality: Multistakeholder robustness tradeoffs for regional water portfolio planning under deep uncertainty. *Water Resources Research*, 50(10), 7692–7713.

Jiang, L. and O'Neill, B.C. (2017). Global urbanization projections for the shared socioeconomic pathways. *Global Environmental Change*, 42, 193–199.

Lempert, R.J. (2002). A new decision sciences for complex systems. *Proceedings of the National Academy of Sciences*, 99(suppl 3), 7309–7313.

O'Neill, B.C., Kriegler, E., Ebi, K.L., Kemp-Benedict, E., Riahi, K., Rothman, D.S., van Ruijven, B.J., van Vuuren, D.P., Birkmann, J., Kok, K., et al. (2017). The roads ahead: Narratives for shared socioeconomic pathways describing world futures in the 21st century. *Global environmental change*, 42, 169–180.

Quinn, J.D., Reed, P.M., Giuliani, M., Castelletti, A., Oyler, J.W., and Nicholas, R.E. (2018). Exploring how changing monsoonal dynamics and human pressures challenge multireservoir management for flood protection, hydropower production, and agricultural water supply. *Water Resources Research*, 54(7), 4638–4662.

Riahi, K., Van Vuuren, D.P., Kriegler, E., Edmonds, J., O'neill, B.C., Fujimori, S., Bauer, N., Calvin, K., Dellink, R., Fricko, O., et al. (2017). The shared socioeconomic pathways and their energy, land use, and greenhouse gas emissions implications: An overview. *Global environmental change*, 42, 153–168.

Smith, M. (1992). *CROPWAT: A computer program for irrigation planning and management*. 46. Food & Agriculture Org.

Valiantzas, J.D. (2006). Simplified versions for the penman evaporation equation using routine weather data. *Journal of Hydrology*, 331(3-4), 690–702.

Van Vuuren, D.P., Edmonds, J., Kainuma, M., Riahi, K., Thomson, A., Hibbard, K., Hurtt, G.C., Kram, T., Krey, V., Lamarque, J.F., et al. (2011). The representative concentration pathways: an overview. *Climatic change*, 109(1), 5–31.

Van Vuuren, D.P., Kriegler, E., O'Neill, B.C., Ebi, K.L., Riahi, K., Carter, T.R., Edmonds, J., Hallegatte, S., Kram, T., Mathur, R., et al. (2014). A new scenario framework for climate change research: scenario matrix architecture. *Climatic Change*, 122(3), 373–386.

Vinca, A., Riahi, K., Rowe, A., and Djilali, N. (2021). Climate-land-energy-water nexus models across scales: progress, gaps and best accessibility practices. *Frontiers in Environmental Science*, 252.

Wilks, D.S. and Wilby, R.L. (1999). The weather generation game: a review of stochastic weather models. *Progress in physical geography*, 23(3), 329–357.

Yu, B., Zhu, T., Breisinger, C., Hai, N.M., et al. (2010). Impacts of climate change on agriculture and policy options for adaptation. *International Food Policy Research Institute (IFPRI)*.